Coherent Combination Method applied to Distributed Acoustic Sensing over Deployed Multicore Fiber

Daniele Orsuti[a], Sterenn Guerrier*[b], Luca Palmieri[a], Élie Awwad[c], Christian Dorize[b], Cristian Antonelli[d], and Antonio Mecozzi[d]
[a]Department of Information Engineering, University of Padova, 35131 Padova, Italy; [b]Nokia Bell Labs, 12 rue Jean Bart, 91300 Massy, France; [c]LTCI, Télécom Paris, Institut Polytechnique de Paris, 91120 Palaiseau, France; [d]Department of Physical and Chemical Sciences, University of L'Aquila, 67100 L'Aquila, Italy

ABSTRACT

From distributed acoustic sensing (DAS) measurements over deployed multi-core fiber (MCF), we discuss several signal processing options to enhance the sensing sensitivity, namely core combination and longitudinal averaging.

Keywords: Distributed Acoustic Sensing, Multicore Fiber, Network monitoring, Digital Signal Processing

1. INTRODUCTION

As we are approaching the limits of single-mode fiber telecommunication systems, research is addressing space-division multiplexing (SDM) transmission. Given the strategic dimension of the communications infrastructure, distributed fiber optic sensing is a capable method to monitor the deployed networks. Its dynamic version, the Distributed Acoustic Sensing (DAS) is a powerful tool to not only detect breaks but also detect and locate vibrational events imparing the cables, without impacting the transmitted data[1]; yet it needs to be extended beyond single-mode fiber monitoring.

Besides, the DAS experiences coherent fading issues, that can be addressed by spatial averaging, selection of high backscatter segments[2], polarization diversity[3], or use of frequency diversity[4]. Core diversity was also addressed recently[5]. In this paper, we perform distributed sensing over two uncoupled cores of a deployed multi-core fiber (MCF) and discuss several signal processing options to enhance the sensing sensitivity, namely core combination and longitudinal averaging. We describe a novel combination algorithm and consider the impact of SNR gap between channels.

2. METHODOLOGY

2.1 MIMO-DAS over deployed multicore fiber

Coherent-MIMO DAS is performed over two successive cores of a deployed 4 uncoupled cores MCF (4UC-MCF), in the city of L'Aquila, Italy[6]. The experimental set-up and deployment configuration are displayed in Fig. 1.

After modulation, the sensing signal is connected to core 1 of the 4UC-MCF through the Fan-In-Fan-Out (FIFO), yielding a 6.3 km sensing path. Looping the output of core 1 back to the input of core 2 yields a 12.6-km overall sensing path, catching the vibrational events in the underground of the city twice. The Coherent-MIMO-DAS transmits dual-polarization signals modulated with bipolar coded sequences (or "codes")[3] at a symbol rate of 50 MBaud with code repetition rate T_{code}=1.3 ms yielding a sensing bandwidth of 385 Hz. Since the speed of light in the fiber is several orders of magnitude above the speed of acoustic waves, we consider that the detected events are the same on both successive cores. The backscattered light is passed through an optical circulator and sent to a dual-polarization coherent receiver, then sampled at a rate of f_{samp}=100 MS/s yielding a theoretical spatial resolution of S_r=1.02 m.

Fig. 1(c) displays the Rayleigh backscattered power from the fiber under test. The pass through the FIFO yields both reflections and connection losses, resulting in a considerably lower SNR for the measurement in core 2. Still, the two cores have independent Rayleigh scatterers distributions, which is of interest for fading mitigation in DAS.

*sterenn.guerrier@nokia-bell-labs.com

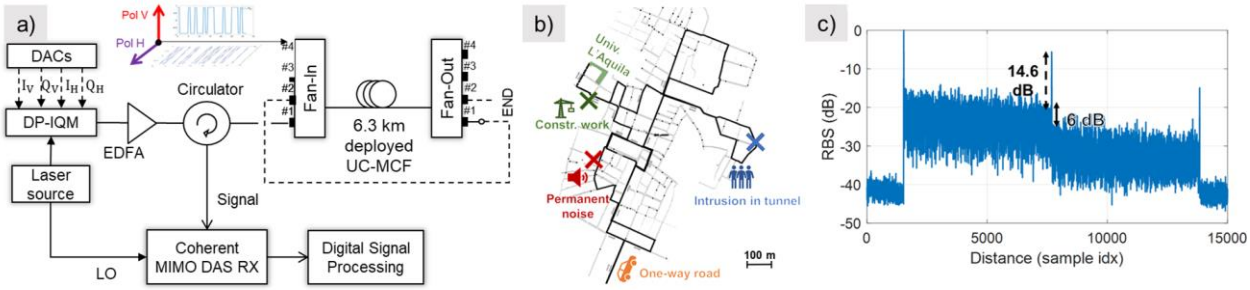

Fig. 1: Experimental set-up. (a) Coherent-MIMO DAS interrogator and MCF connection set-up. DP-IQM: Dual-pol. I/Q modulator; DACs: Digital-to-Analog Converters (b) Map of the 6.3-km MCF testbed in L'Aquila (markers to point construction works, permanent noise, road traffic, and intentionally produced perturbations in the tunnel) (c) Rayleigh backscattered intensity from two consecutive core interrogation.

2.2 Smart core combination principle

The cores of the MCF are subject to the same perturbations and have distinct and uncorrelated Rayleigh fading signatures[7]; therefore, they act as independent measurement channels whose information can be combined to reduce signal fading. The information gathered by the cores needs to be optimally combined, or averaged, into a single result. Let the Rayleigh backscattered trace of core c $(c = 1, 2)$ measured at N_T consecutive time samples t_n $(n = 1, \dots, N_T)$ and at the arbitrary longitudinal sample, z_k, be denoted as $r_c(t_n)$. Despite being affected by the same perturbations, the complex traces $r_c(t_n)$ have an unpredictable phase offset, which prevents their direct averaging. This phase offset must be removed before averaging, so as to coherently combine the traces.

A well-known technique for achieving coherent averaging is the so called rotated-vector-sum (RVS) method[8], which selects an arbitrary reference time sample, t_1, and applies a rigid phase rotation to the traces $r_c(t_n)$ so that $r_c(t_1)$ has zero phase for every c. This way, the RVS method aligns the phases of the traces while preserving the temporal phase variation caused by perturbations. Nonetheless, no indication is given for selecting the reference time t_1, and an incorrect choice can compromise the alignment of the traces. To address this issue, in Ref. [9], the alignment is performed observing the entire temporal window of size N_T samples, rather than relying just on a single time sample; the phase offset is determined by solving a least-mean-square (LMS) error problem, which yields the optimum phase offset for aligning the traces. This LMS approach has been shown to provide superior performance compared to the RVS method[9]; moreover, the LMS problem can be defined to give more importance to higher amplitude samples, making it well-suited to deal with the SNR gap between the cores in our experiment. The LMS method, in its general settings, i.e., when aligning an arbitrary number of traces, consists of the following steps. First, the trace with the highest energy within the time window N_T is selected as the reference trace; then, each trace is aligned to the reference trace solving a relative LMS problem. Let $\bar{r}(t_n)$ be the reference trace according to the highest-energy criterion; the phase offset that aligns $r_c(t_n)$ to $\bar{r}(t_n)$, denoted as ϕ_c, is determined by seeking for ϕ_c that minimizes the cost function $C = \sum_n w_n |\bar{r}(t_n) - r_c(t_n) \exp(j\phi_c)|^2$, where the weight factor $w_n = |\bar{r}(t_n)||r_c(t_n)|$ is selected to give more importance to higher amplitude samples. Setting the derivative of the cost function equal to zero gives the solution of the relative LMS problem as

$$\phi_c = \arg\{\textstyle\sum_n w_n\, \bar{r}^*(t_n) r_c\,(t_n)\}. \tag{1}$$

The optimum phase offset given by Eq. (1) is used to perform a rigid phase rotation of $r_c(t_n)$ before averaging. The width of temporal window N_T over which the phase offset is estimated needs to be selected sufficiently wide to effectively detect the highest-energy trace and accurately estimate the phase offset.

So far, we have discussed how to exploit the information diversity carried by the cores of the MCF to reduce signal fading. This approach can be generalized to exploit the information diversity carried by the z-samples of the measured Rayleigh backscattered trace, as detailed in what follows. In the experimental setting considered in this work, the Rayleigh backscattered trace is measured with a spatial resolution of 1.02 m, while the deployed MCF is exposed to perturbation that spatially spread over several meters; these parameters suggest that subsequent z-samples experience a similar temporal phase variation. Therefore, the information carried by a small number of subsequent z-samples, N_Z, can be combined to exploit longitudinal diversity at the cost of a marginal degradation of the spatial resolution. Actually, subsequent z-samples can be treated as independent measurement channels of the same event, to which coherent averaging can be applied to reduce signal fading. In order to minimize the degradation of the spatial resolution, here, we consider only two subsequent

sample, i.e., N_Z=2; this means that, at the arbitrary position z_k, for each core, we also consider the subsequent sample z_{k+1} to obtain a total of 4 traces: $r_c(z_k, t_n)$ and $r_c(z_{k+1}, t_n)$, with $c = 1, 2$. These traces are coherently averaged with the above described LMS method; the effective spatial resolution after averaging results in $S_r^{eff} = S_r \cdot N_Z$=2.04 m. This longitudinal average procedure can be readily extended to account for a higher number of subsequent z-samples, yet at the cost of a worse effective spatial resolution.

3. RESULTS AND DISCUSSION

3.1 Core combination performance

To determine the improvement offered by core combination, we evaluate the standard deviation of the local phase variation signal for both the individual cores and the LMS average of the cores over an interrogation of approximately 1-minute duration. We expect the LMS average of the cores to reduce the number of fading points, thus decreasing the noise floor, and, consequently, improving the detection of events along the fiber.

Figure 2(a) shows the results obtained when computing the standard deviation over the entire acquisition time; whereas Fig. 2(b) shows the results obtained when calculating the standard deviation over a sliding window of 200 ms, which generates a time-distance map of the events occurring along the fiber. In the map, the phase variations are mapped into logscale to enhance the color contrast: brighter points correspond to stronger variations, dark points to silent zones. The markers on top of the figures denote the event type, which is assigned consistently with the testbed map shown Fig. 1(b). In the figures, N_Z=1 corresponds to the case where longitudinal diversity is not exploited.

The 1-minute-long acquisition was processed in chunks of N_T=100 samples (i.e., 130 ms), over which the phase offsets are computed according to Eq. (1); consecutive chunks overlap by 1 time sample so to retain the continuity of the phase signal.

From the 1D plots in Fig. 2(a), it can be observed that core 2 has significantly higher standard deviation values than core 1 due to the FIFO losses; yet, the LMS average of core 1 and core 2 for N_Z=1 results in a moderate reduction of the noise floor compared to core 1, thus indicating the successful combination of the two cores. The best performance is obtained when exploiting both core diversity and longitudinal diversity with N_Z= 2, which yields a significant reduction of the noise floor. The 2D maps in Fig. 2(b) further confirm the improvement offered by coherent averaging and highlight the events along the fiber path. Besides several motionless disturbances, which appear as vertical lines in the maps, it is possible to observe oblique waterfall traces (enclosed by a red rectangle in the figure) corresponding to a moving vehicle on a section of fiber installed in a round trip path under a roadway (note that the two slopes are not perfectly mirrored as the tunnel is actually shifted by an angle θ= ~30° relatively to the road).

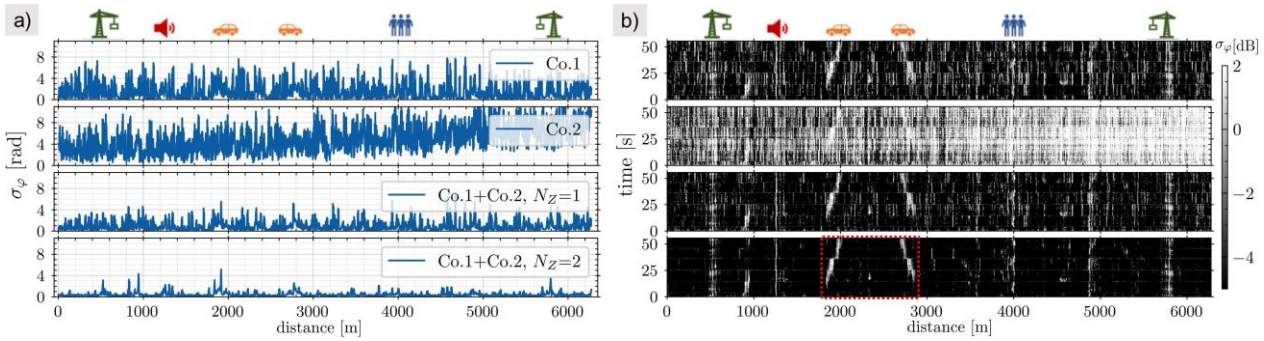

Fig. 2: Core combination results. (a) Standard deviation of phase variations calculated over a 1-minute-long acquisition for single cores (Co.1 and Co.2) and LMS average of the cores (Co.1+Co.2). (b) Time-distance map of phase variations corresponding to the curves in (a), with top markers for identified events and red rectangle for moving vehicles related events. N_Z denotes the number of consecutive z-samples included in the averaging procedure.

3.2 Longitudinal averaging performance

It is interesting to investigate the performance improvement that can be obtained by exploiting longitudinal diversity alone; to this end, we consider each core separately and apply the coherent average along the longitudinal direction. In contrast to Section 3.1, where the LMS average is computed both across the cores and across the z-axis, limiting the average only

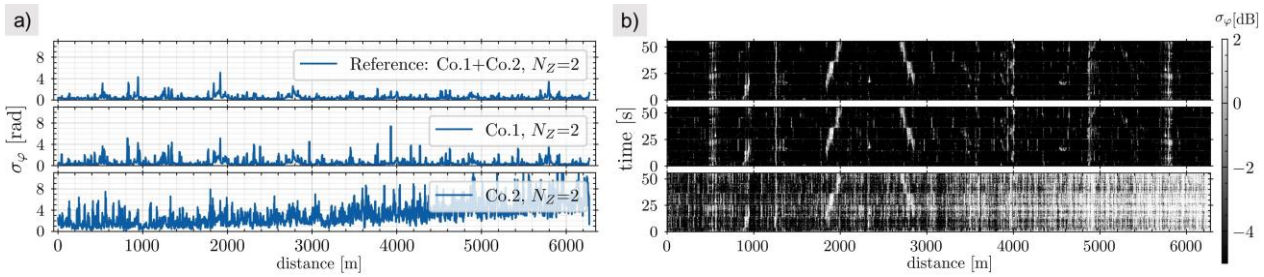

Fig. 3: Longitudinal averaging results. (a) Standard deviation of phase variations calculated over a 1-minute-long acquisition exploiting both core diversity and longitudinal diversity (Co.1+Co.2) and exploiting longitudinal diversity only (Co.1 and Co.2). (b) Time-distance map of phase variations corresponding to the curves in (a). N_Z=2 denotes that two consecutive z-sample are considered for longitudinal averaging.

to the z-axis allows to distinguish the improvement offered by core diversity from the improvement offered by longitudinal diversity. The results of this comparison are shown in Fig. 3, where we also include, for reference, the results obtained in Section 3.1 when averaging both across the cores and across the z-axis (labeled as "Reference" in the figure legend). It can be observed that longitudinal averaging alone greatly decreases the noise floor in both cores. Notably, after longitudinal averaging, most of the events along the fiber can be easily identified in core 2, which was not possible in Fig. 2(b) due to the high noise floor level. Furthermore, it can be observed that the longitudinal average of core 1 offers similar performance, slightly worse, compared to the case in which core diversity is also considered. This can be attributed to the higher intensity backscattered trace of core 1, which causes the contribution of core 2 to be only marginal when extending the average along the z-axis.

In conclusion, we conducted DAS measurements over a multi-core fiber deployed under the city of L'Aquila, Italy. We introduced a novel coherent averaging method that exploits both the information diversity carried by the cores and the information diversity carried by the z-samples of backscattered trace to effectively reduce signal fading. The proposed method significantly improves the SNR with only a minimal degradation of the spatial resolution, allowing for successful localization and identification of traffic-related events and construction works events along the fiber path.

REFERENCES

[1] S. Guerrier *et al.*, "Vibration Detection and Localization in Buried Fiber Cable after 80km of SSMF using Digital Coherent Sensing System with Co-Propagating 600Gb/s WDM Channels," in *Optical Fiber Communication Conference (OFC) 2022, paper M2F.3*, Mar. 2022.

[2] E. Awwad, *et al.*, "Efficient Multi-Event Localization from Rayleigh Backscattering in Phase-Sensitive OTDR Systems," in *Optical Sensors and Sensing Congress*, San Jose, California, 2019, p. EW6A.2.

[3] S. Guerrier, *et al.*, "Introducing coherent MIMO sensing, a fading-resilient, polarization-independent approach to ϕ-OTDR," Opt. Express, vol. 28, no. 14, p. 21081, Jul. 2020

[4] S. Guerrier, *et al.*, "A fully digital MIMO-OFDM scheme for fading mitigation in Coherent Δφ-OTDR," Optics Express, Oct. 2021.

[5] Y. Feng *et al.*, "Multicore Fiber Enabled Fading Suppression in φ-OFDR Based High Resolution Quantitative DVS," *IEEE Photonics Technology Letters*, vol. 34, no. 19, pp. 1026–1029, Oct. 2022.

[6] S. Guerrier *et. al*, 'Field Trial of High Resolution Multi-Dimensional Fiber Sensing over Multicore Fiber with Construction Work Localization using Advanced MIMO-DAS', in *Optical Fiber Communication Conference*, paper W1J5, San Diego, March 2023.

[7] L. Palmieri, *et al.*, "Rayleigh-Based Distributed Optical Fiber Sensing," *Sensors*, vol. 22, no. 18, p. 6811, Sep. 2022.

[8] D. Chen, *et al.*, "Phase-detection distributed fiber-optic vibration sensor without fading-noise based on time-gated digital OFDR," *Opt. Express*, vol. 25, no. 7, p. 8315, Apr. 2017.

[9] D. Orsuti *et al.*, "Analysis of distributed acoustic sensing in multimode fibers based on heterodyne optical time domain reflectometry," in *27th International Conference on Optical Fiber Sensors*, Alexandria, Virginia, 2022, p. Th4.27.